Numerical Simulation of Gravity Current Propagation in a Compressible Atmosphere

M.V. Shokurov, N.Yu. Germankova

Marine Hydrophysical Institute, Russian Academy of Sciences, Sevastopol, Russian Federation
e-mail: shokurov.m@gmail.com, loogaru9@rambler.ru

Gravity current is one of the components of sea breeze circulation. For investigation of sea breeze circulation propagation of a gravity current in the atmosphere is numerically modeled using a two-dimensional hydrodynamic model allowing for compressibility. The result consists in a detailed description of development and propagation of a gravity current at the stage when the front speed is constant. Characteristic features of the structure of gravity current – front, «head», Kelvin-Helmholtz vortices − are noted. The dynamic characteristics of gravity current such as propagation velocity of front, current height, buoyancy deficit in the gravity current are determined. The dependence of the flow dynamic characteristics upon two following parameters is studied: the initial difference between potential temperatures of the cold air pool and the environment, and the initial height of the cold pool. Dimensionless front velocity (Froude number Fr) is calculated by three methods using characteristic heights of the current "head" and "body" which is located behind the "head", and the cold pool initial height. The calculations show that in the first approximation Fr calculated from the gravity flow height, is actually a universal constant approximately equal to 1. More detailed analysis shows that Fr and the gravity current height are weakly dependent upon the ratio between the cold pool initial height and the atmosphere thickness. The conclusion is consistent with the results of other studies.

Keywords: gravity current, numerical simulation, Froude number.

DOI: 10.22449/1573-160X-2015-4-53-65

1. Introduction

Gravity or density currents induced by the horizontal density gradients are widely distributed in the ocean and the atmosphere. They can propagate both on the horizontal and inclined underlying surface, on the ocean free surface and also as intrusions between the layers of different density in a stratified fluid. The differing fluid densities can be conditioned by difference in temperature and salinity in the ocean and fine impurity or suspension concentrations in the atmosphere and the ocean. Typical examples of the gravity currents in the atmosphere are sea breezes, spreading of cold air formed in the thunderstorm clouds over the land surface, cold mesoscale fronts, mountain-valley slope winds, dust storms, snow avalanches and mudslides on the mountain slopes, and lava and pyroclastic flows at volcanic eruptions. As for the ocean, the characteristic examples of the gravity currents are distribution of estuary freshwater in salt seawater, turbidity flows in the underwater canyons, water-exchange between the basins through narrow straits such as the Bosporus and Gibraltar, and so on [1].

A gravity current in the atmosphere is one of the components of breeze circulation. Urgency of its detailed study is conditioned by significant influence of breeze upon local weather and climate. The motion of cold sea air to land at typical synoptic conditions takes on the character of a gravity current including formation of a sharp breeze front.

The gravity currents are traditionally studied by means of laboratory experiments [2 – 4]. In recent years, numerical simulation of gravity currents was also widely used [1, 5, 6]. Analysis of laboratory and numerical experiments, and application of analytical results for simplifying formulation of the problem [4, 7] has resulted in creating a rather developed, though not completed, theory of gravity currents [8].

A classic experiment for studying gravity currents is total or partial lock exchange [3 – 5]. Considered is a bulk divided by a partition into two parts which are filled with the fluids of different densities. After the partition is raised the denser fluid propagates to the area where the fluid is lighter. In this experiment the gravity current goes through several stages of development. At the first stage it accelerates, then the current is transferred into the second stage when the front speed is constant and, at last, into the third one which is the inertial phase. At the last stage the viscosity effect gains in importance and the current continues to spread in the viscous phase. The second stage with constant speed is of special interest for studying the breeze circulation as it takes place in nature in typical synoptic conditions. The majority of theoretical works is dedicated to investigation of this stage.

The gravity current with constant front speed can be considered steady. Using the laws of the mass, momentum and energy conservation, i.e. constancy of their flows along the current, one can obtain dependence of the front propagation speed and the gravity current height upon the initial parameters of the problem: the buoyancy initial deficit and the cold air pool height. Such an approach has led to defining an important parameter – the Froude number (Fr) connecting the current propagation speed with its height and deficit of the heavy fluid buoyancy [7, 8].

To consider the gravity currents' evolution in more real situations, numerical simulation with various kinds of the motion equations' simplifications are used. The simplest equations' system suitable for simulating the gravity current is the system of shallow water equations [2, 5, 8]. These equations can be applied when the gravity current horizontal scale strongly exceeds the vertical scale and the vertical acceleration can be neglected in contrast to the horizontal one, i.e. when the hydrostatic approximation is fulfilled. These conditions are not satisfied at the initial stage of acceleration during the lock exchange and also around the "head" and front of the gravity current at any time. However, the shallow water equations fairly well describe propagation of the gravity currents, if the boundary condition connecting the front speed and the current height is preset on the front. This very boundary condition can be obtained from the experiments, the analytical theory or more sophisticated numerical models.

The next in complexity class of the numerical models intended for studying the gravity currents is the two-dimensional models based on full hydrodynamic equations [5, 6]. They are used in a vertical plane normal to the gravity current front since the basic dynamic processes in such a current are two-dimensional. At the first stages the motion equations for an incompressible fluid were applied allowing for the Boussinesq approximation; it is quite acceptable for the gravity currents observed in the ocean or in rather thin layers of the lower atmosphere. The system of motion equations taking into account compressibility in the so-called inelastic form was used with time for simulating the atmospheric gravity currents. The characteristic speeds of the process under study are assumed to be significantly lower than the acoustic speed; therefore the gravity-acoustic waves can be neglected and removed from the motion equations. At present the majority of the researchers use full non-hydrostatic equations (describing incompressible atmosphere) in which the gravity-acoustic waves are taken into account.

The shallow water equations are not a suitable tool for studying the breeze gravity currents. Primarily, it is due to the fact that the real atmosphere has a fairly complex stratification and the background synoptic wind profile with the vertical velocity shear. These features of the real atmosphere can not take into account in the shallow water model. At the same time it is known that they can lead to the important effects such as the internal waves' generation or development of strong convection over the breeze front. Hence, a more appropriate instrument is a full two-dimensional model. Application of the Boussinesq or incompressibility approximations also restricts the class of the considered problems by small amplitude of the density disturbance and small vertical scale.

The purpose of this paper is to develop a high-quality two-dimensional numerical atmospheric model with high spatial resolution based on full equations of motion and heat transfer allowing for compressibility. It is intended for numerical simulation of the breeze gravity currents. The numerical simulation should result in full and detailed description of the gravity current structure and dynamics, and also in defining dependence of the gravity current basic characteristics – the current height and the front propagation speed – upon the initial parameters of the problem. Section 2 represents brief description of the applied model and its finite-difference realization, section 3 – formulation of the problem, description of the numerical experiments and the method of their realization, section 4 – the simulation results. The conclusions drawn from the simulation results are given in the final section of the paper.

2. Description of the model

The model equations.

It was already said that in order to understand and describe quantitatively the main features of the atmospheric gravity currents, the two-dimensional models can be rather successfully used. It is confirmed by numerous works on modeling the atmosphere processes the basis of which consists in a gravity current [1, 5, 6]. In this paper the two-dimensional model of a compressible atmosphere based on the full equations of motion and heat transfer was used for studying. The model equations are written in a vertical plane normal to the gravity current front with the coordinates x and z. The equation system consists of four prognostic equations: the motion equations for the velocity components (u, w), the equation for dimensionless pressure (π) deduced from the continuity equation, and the heat transfer equation for the potential temperature (θ). The characteristic time scale of the process of the breeze gravity current formation is ~1 h, therefore the Coriolis force can be neglected. The turbulent transport is the important process in the atmospheric boundary layer. In this paper we have chosen the simplest parameterization of this process: constant coefficients of viscosity and heat conductivity. The equations including turbulent viscosity and heat conductivity (without taking into account the Earth's rotation) are as follows:

$$\frac{\partial w}{\partial t} = -\frac{\partial uw}{\partial x} - \frac{1}{\overline{\rho}}\frac{\partial \overline{\rho} ww}{\partial z} - C_p \overline{\theta}\frac{\partial \pi'}{\partial z} + g\frac{\theta'}{\overline{\theta}} + k_x \frac{\partial^2 w}{\partial x^2} + k_z \frac{\partial^2 w}{\partial z^2},$$

$$\frac{\partial u}{\partial t} = -\frac{\partial uu}{\partial x} - \frac{1}{\overline{\rho}}\frac{\partial \overline{\rho} uw}{\partial z} - C_p \overline{\theta}\frac{\partial \pi'}{\partial x} + k_x \frac{\partial^2 u}{\partial x^2} + k_z \frac{\partial^2 u'}{\partial z^2},$$

$$\frac{\partial \pi'}{\partial t} = -\frac{\bar{c}_s^2}{\bar{\rho} C_p \bar{\theta}^2}\left[\bar{\rho}\bar{\theta}\frac{\partial u}{\partial x} + \frac{\partial \bar{\rho}\bar{\theta} w}{\partial z}\right] + k_x \frac{\partial^2 \pi'}{\partial x^2} + k_z \frac{\partial^2 \pi'}{\partial z^2},$$

$$\frac{\partial \theta'}{\partial t} = -\frac{1}{\rho}\left(\frac{\partial \rho u \theta'}{\partial x} + \frac{\partial \rho w \theta'}{\partial z} + \frac{\partial \rho w \bar{\theta}}{\partial z}\right) + k_x \frac{\partial^2 \theta'}{\partial x^2} + k_z \frac{\partial^2 \theta'}{\partial z^2}, \qquad (1)$$

w——here ρ is the air density; C_p is the specific heat at constant pressure for dry air; k_x, k_z are the coefficients of turbulent viscosity and heat conductivity; g is the free fall acceleration. The equation system (1) is written for the full variables ($u = \bar{u} + u'$). The variables with a prime correspond to the disturbances, those with a line – to the basic state which is preset at the initial time moment.

The dimensionless pressure (the Exner function) is defined in a following way:

$$\pi = \left[\frac{p}{p_0}\right]^{\frac{R_d}{C_p}}, \qquad (2)$$

where p is pressure, mbar; p_0 is the pressure at the sea level (p_0 = 1000 mbar); R_d is the universal gas constant for dry air (R_d = 287 J/kg). Some terms are excluded from consideration due to their insignificant influence on the phenomenon under examination.

The equation system (1) was successfully used in simulating deep convection and cold air outflow formed in a storm cloud, and other atmospheric processes. More detailed description of the applied system is given in [6, 9]. In the present variant of the model, the atmospheric humidity, the cloudiness and also the radiation transfer in the visible and long wave ranges are not taken into account.

Boundary conditions.

The basic requirement in choosing the boundary conditions consists in eliminating the boundaries' possible effect on the process in question.

In the problem of lock exchange, for the finite pool of cold air, due to symmetry, it is suitable to choose the left boundary of the area in the cold pool center and to consider it a solid wall. Thus, the speed horizontal component is equated with to zero on this boundary (rigid boundary). On the right boundary the radiation condition intended for preventing possible disturbances' reflection is used for this variable.

On the lower and upper boundaries the free-slip condition (i. e. zero shear) on the underlying surface is applied to the speed horizontal component; it is traditionally used to study gravity currents. It is connected with the fact that the no-slip condition on the lower boundary complicates the current structure, leads to development of the boundary layer within the gravity current and, as a result, to its slowing down conditioned by viscosity. The free-slip condition is introduced just to eliminate the viscosity effect and to simplify the results' analysis.

For the speed vertical component, the rigid boundaries**,** i. e. zero values, are chosen on the lower and upper boundaries. On the lateral boundaries, the speed zero shear condition is used for this value as a boundary condition. On all four boundaries, for potential temperature and pressure, the zero gradient condition, i. e. absence of heat and mass inflows through the boundaries, is used.

Finite-difference realization.

Finite-difference realization of the model implies application of the spatial grid in which the scalar variables (potential temperature and pressure) are calculated in the cell center, the speed horizontal component – on the cell lateral sides, and the speed vertical component – on its upper and lower sides. Transfer of the variables from the center to the cell side, or vice versa, when it is required for the finite-difference approximation of various terms of the model equations, is done by means of horizontal and vertical interpolation.

In numerical simulation, two schemes with central differences in space and in time (the latter is called "leapfrog") are used in all four equations to describe advection. The second order central differences in space and the explicit scheme – in time are applied for describing viscosity and heat conductivity.

Application of the central differences for calculating advection results in computational dispersion on small scales. However this drawback of the numerical scheme is not significant since the small scale disturbances are effectively suppressed by turbulent viscosity and heat conductivity with constant identical coefficients' values. Over the horizon $k_x = 100$ m^2/s and over the vertical $k_z = 15$ m^2/s.

3. Methods of numerical experiments

In the present paper we have chosen the simplest formulation of the problem – propagation of the gravity current from the limited bulk of cold air to the neutral environment. The effect of stratification and wind shear in the surrounding atmosphere will be investigated in details in the subsequent papers.

The dimensions of the considered area are $L_x = 50$ km over the horizon and $H = 5$ km over the vertical. The horizontal and vertical grid steps are the same and equal to $\Delta x = \Delta z = 50$ m. Thus, the grid' dimensions are $N_x = 1000$ nodes, $N_z = 100$ nodes. Such a high resolution is chosen to make the gravity current description more detailed. The step in time Δt is equal to 0.05 in order to fulfill two criteria: the CFL one for advection and the criterion of the explicit scheme stability for viscosity and heat conductivity. The calculation is performed up to the time moment when the gravity current reaches the right boundary of the area under consideration.

The isentropic atmosphere which is in the hydrostatic equilibrium is taken as a basic state at the initial moment. At that the fields of potential temperature and pressure are horizontally uniform. The wind speed is assumed to be zero.

The pressure and the density in the basic satate are calculated as follows:

$$\frac{d\overline{\pi}}{dz} = -\frac{g}{\overline{\theta} C_p}, \tag{3}$$

$$\overline{\rho} = \frac{p_0 \overline{\pi}^{\frac{C_v}{R_d}}}{\overline{\theta} R_d}, \tag{4}$$

$$C_v = C_p - R_d, \tag{5}$$

where C_v is the specific heat at the constant volume.

To preset the initial disturbance, we use the area with 20 km length in which cold air is present. Further we call this area the cold pool.

Five numerical experiments were performed (Table. 1). In the first three ones, the same values of the potential temperature differences ($\Delta\theta = 5$ K) are preset; at

that the height of the released volume D equal to 1; 1.5 and 2 km changes. In two other experiments, the cold area height is assumed to be constant (D = 1.5 km), and the initial difference of potential temperatures takes on different values (2 and 8 K).

4. Results

Structure of the gravity current.

In all the experiments, after the initial state is preset the motion of the heavier air from the cold pool to the surrounding atmosphere is observed. Immediately after the cold air is released, it accelerates during 1 – 2 minutes, after that the gravity current begins to move at a constant speed.

Let us consider in details distribution of the potential temperature disturbances θ', two speed components u, w and pressure for the time moment t = 16 min after the integration in the experiment begins. The initial height of the released cold air volume D = 2 km, the initial temperature difference $\Delta\theta$ = 5 K.

Fig. 1 represents the potential temperature disturbance. The front with large horizontal temperature gradient is formed with time in the fore-part of the current. Behind the front, the gravity current "head" is formed, it is followed by the well-pronounced height minimum. Further the "body" is located in which gradual increase of the cold air layer thickness is observed.

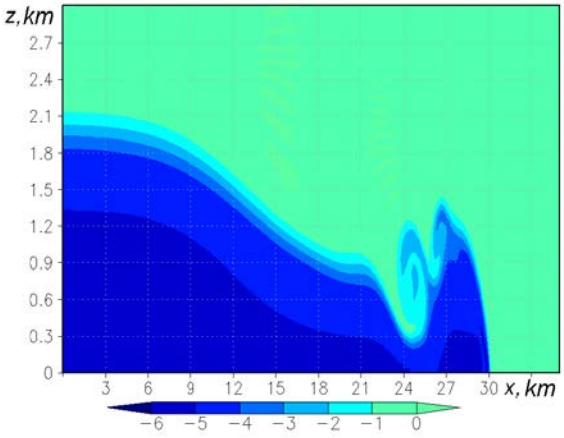

Fig. 1. Profile of the potential temperature disturbance (K) at t = 16 min

The current motion is accompanied by its gradual diffusion due to the effect of the turbulent heat conductivity that results in decrease of the density gradient on the air masses' interface. In the upper part of the "head" observed are the vortices induced by the Kelvin-Helmholtz instability which develops on the boundary between two air masses of different density resulting from the speed shear on the interface. Having been formed, the vortices move towards the gravity current "body".

Fig. 2 shows distribution of the wind speed horizontal component and the current lines. In the horizontal speed field, observed is gradual acceleration of the air motion from the cold pool (where its speed is zero) towards the gravity current

"head" where the air speed is 12 – 15 m/s. Behind the gravity current "head" where the height is minimum, the air speed attains even higher values – 18 m/s. In the course of time more and more cold air becomes involved in the motion, and, at last, all the air that was inside the initial cold pool comes into motion.

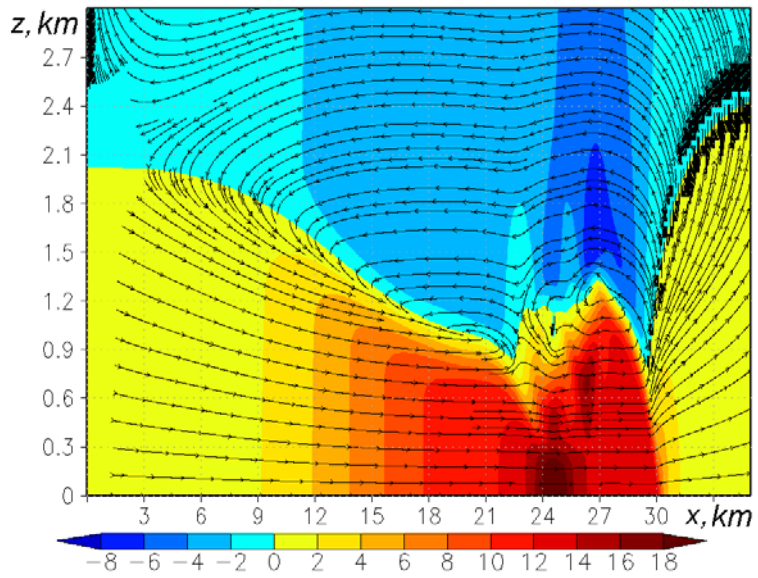

Fig. 2. Profile of the horizontal wind speed (shown by color) and distribution of the current lines (lines with arrows) at t = 16 min

Propagation of the gravity current is accompanied by formation of a warm return current. Its height in the upper part of the considered area is a few times as much than that of the very gravity current, hence the speed in the upper current is approximately two times as less than that in the lower one. While the gravity current develops, the horizontal convergence before its front is observed; it results in rapid air elevation before the front and in its lowering behind the current's "head".

Between the cold air gravity current and the warm air return current, a thin layer with a strong speed shear is clearly seen (Fig. 2). The result of this shear is that the Kelvin-Helmholtz vortices are formed above the "head".

Fig. 3 shows distribution of the pressure disturbance which is mainly of a hydrostatic character; it is confirmed by the increased pressure in the cold pool. Pressure in this part of the examined area decreases with time. However, there are pressure disturbances which are related to the non-hydrostatic effects like high values of the vertical speed in the front area and abrupt speed changes in the vortices. The pressure lowering connected with the vortex rotation speed by the cyclostrophic balance equation is observed in the area of the current "head" where the Kelvin-Helmholtz vortices are formed and in the very vortices [6].

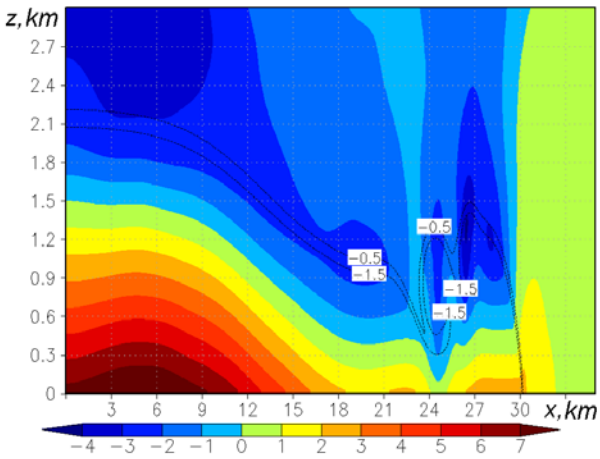

Fig. 3. Profile of pressure (× 10^4, shown by color) and potential temperature disturbances –0.5 and –1.5 K (indicated by isolines) at t = 16 min

Fig. 4 represents the plot (traditionally used in gravity currents' studies) with the coordinates x, t (the Hovmöller plot) describing evolution of the potential temperature disturbances at the 100 m height in the experiment with the cold area initial height 2 km and the temperature difference 5 K. Propagation of the gravity current front is represented in a form of the distinct boundary separating the air masses with different potential temperatures. It is seen that throughout the whole experiment, the front moves at a constant speed, and the acceleration stage in the beginning of the motion takes only 1 – 2 min. Also inside the cold air area (on the Hovmöller plot), the narrow strips of the increased temperature are observed. It is due to formation of the Kelvin – Helmholts vortices which mix two air masses that leads to the cold air gradual heating.

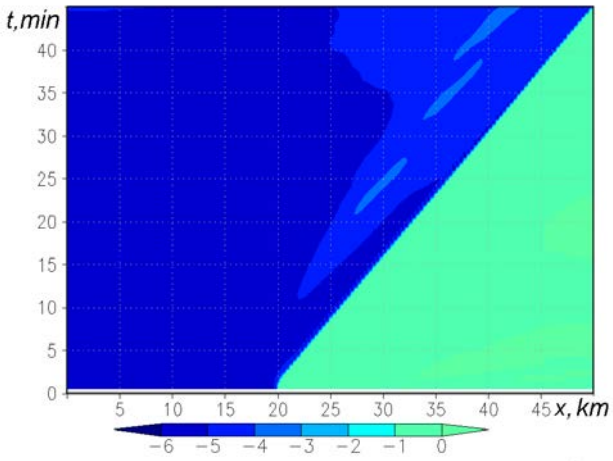

Fig. 4. The Hovmöller plot describing evolution of the potential temperature disturbance on the height 100 m

Determination of the gravity current characteristics.

Let us define the gravity current basic characteristics obtained by numerical simulation in five experiments. These characteristics usually include the speed of the current front propagation (U), the gravity current height (h) and the reduced gravity (g') or the buoyancy deficit.

It is also common to consider the dimensionless Froude number composed of these three characteristics. It permits to describe quantitatively the gravity current distribution:

$$\mathrm{Fr}_h = \frac{U}{\sqrt{g'h}}, \tag{6}$$

where U is determined by the least squares method using the data on the front position on each successive step in time. g' is defined in the following way:

$$g' = \frac{g(\theta_0 - \theta)}{\theta_0}, \tag{7}$$

where θ_0 is the initial potential temperature of the surrounding fluid (θ_0 = 300 K); θ is the potential temperature of the cold fluid area.

The above formulae can be applied to two immiscible air masses, but in our case the temperature is distributed continuously. Therefore the following method for determining g' and h is applied. The value in the denominator of formula (6) is obtained by integrating the buoyancy deficit over the vertical:

$$g'h(x,t) = \int_0^H g\left(\frac{\theta_0 - \theta}{\theta_0}\right)dz. \tag{8}$$

The height of the gravity current is calculated as follows:

$$h(x,t) = \frac{1}{g'_0} g'h(x,t), \tag{9}$$

where $g'_0 = \frac{g\Delta\theta}{\theta_0}$ is the initial buoyancy deficit.

These two calculated values depend on x and t. In order to calculate the united integral characteristics describing the gravity current in general, they are to be averaged over a certain part of the gravity current.

In scientific literature there is no consensus on the height which is to be used for calculating the Froude number. That is why in literature the Fr values vary significantly depending on the applied characteristic height.

In this paper calculation of the Fr value implies application of two characteristic current heights; they differ in choice of the averaging area on the x axis. The first one is the current "head" height (h_1) which is averaged over the area width starting from the current front up to the minimum height located behind the current "head". The second characteristic height is the current "body" height (h_2). During calculation it is averaged from the minimum current height up to the right boundary of the cold air initial area.

To obtain more accurate values, the heights h_1 and h_2, after being calculated, are also averaged over time. The moment when the height minimum is formed within the current structure and it is outside the initially preset cold air area, is considered to be the initial one. The final moment of time averaging is the end of the model calculation.

In the third variant of Fr calculation, the height of the initial cold pool *D* is used as the characteristic height, and the initial buoyancy deficit g_0' – as the reduced gravity [4, 5]:

$$\mathrm{Fr}_D = \frac{U}{\sqrt{g_0' D}}. \tag{10}$$

At such a calculation of the Froude number, there is no uncertainty in choice of averaging over the vertical, the horizontal and time since the Fr number depends on the exactly known initial values of D and g_0'.

Table 1 represents the gravity currents' integral characteristics calculated based on the results of five numerical experiments. At that the height of the current "head" h_1 was used as the characteristic height. The first column shows the values of the cold area initial height *D*, the second – the values of the temperature initial differences between the surrounding air and the cold area $\Delta\theta$. The current front speed *U*, the root values from the integral reduced gravity $g'h_1$, the height h_1 calculated using the current "head" are represented in the third, fourth and fifth columns, respectively. The sixth column shows the Froude numbers Fr_{h_1} calculated based on the results of the numerical experiments.

Table 1. The gravity current characteristics preset in the initial conditions (columns 1 and 2) and calculated (columns 3 – 7) in the numerical experiments using the current "head" height h_1

D, km	$\Delta\theta$, K	*U*, m/s	$\sqrt{g'h_1}$, m/s	h_1, km	Fr_{h_1}	$\mathrm{Fr}_{\mathrm{theor}}$
1	5	8.6	7.7	0.37	1.1	1.3
1.5	5	10	9.7	0.58	1.1	1.2
2	5	11	11	0.80	1	1.1
1.5	2	6.4	6.2	0.58	1	1.2
1.5	8	12	12	0.58	1	1.2

Table 2 represents integral characteristics of the gravity currents resulted from five numerical experiments and those of the Froude number calculated using the current "body" height h_2. The designations are the same as in Table 1.

The third version of the Froude number calculation using the first three numerical experiments is shown in Table. 3. The designations in the first three columns of all the tables are same, the fourth column of Table 3 gives the ratio of the pool height to the atmosphere thickness *D*/*H*, the fifth column – the reduced gravity g_0', the sixth column – the root values from the integral reduced gravity $g_0'D$, the se-

venth column – the Froude number Fr_D and the eighth column – the ratio of the "head" height h_1 to the cold pool height D.

Table 2. The gravity current characteristics preset in the initial conditions (columns 1 and 2) and calculated (columns 3 – 7) in the numerical experiments using the current "body" height h_2

D, km	$\Delta\theta$, K	U, m/s	$\sqrt{g'h_2}$, m/s	h_2, km	Fr_{h_2}	$\mathrm{Fr}_{\mathrm{theor}}$
1	5	8.6	8.4	0.43	1	1.2
1.5	5	10	9.7	0.58	1.1	1.2
2	5	11	11	0.77	1	1.4
1.5	2	6.4	6.4	0.62	1	1.2
1.5	8	12	12	0.57	1	1.5

Table 3. The gravity current characteristics preset in the initial conditions (columns 1 and 2) and calculated (columns 3 – 7) in the numerical experiments using the cold pool height D

D, km	$\Delta\theta$, K	U, m/s	D/H	g'_0, m/s^2	$\sqrt{g'_0 D}$, m/s	Fr_D	h_1/D
1	5	8.6	0.2	0.16	13	0.66	0.37
1.5	5	10	0.3	0.16	15	0.65	0.39
2	5	11	0.4	0.16	18	0.61	0.40

Interpretation of the obtained results and comparison with the results of other authors.

First of all it should be noted that the Froude number in the sixth column of tables 1 and 2 calculated from the values of the current heights h_1 or h_2 does not depend on choice of the initial conditions D and $\Delta\theta$ and takes on the same value $\mathrm{Fr}_h \approx 1$ in all five experiments. This result confirms the well-known hypothesis that the local Fr number describing relation between the gravity current front speed, its height and buoyancy deficit is a universal constant. The local (or frontal) Froude number is conditioned only by local dynamics in the area of a gravity current "head" and does not depend on the current history, size and position of its source – the cold reservoir. One can say that the very shape of a gravity current is universal. It is true only for the stage of the gravity current propagation characterized by the constant front speed when the current can be considered stable.

The results of numerical simulations carried out by other authors [5, 6] and also those of laboratory experiments [2, 4] support the hypothesis on universality of the local Froude number. But as for the very value of this universal constant, it is very strongly spread from the values smaller than 1 to those exceeding 1. It is primarily related to choice of the gravity current characteristic height the values of which in scientific literature are different.

According to the Karman theory [7], the local Fr theoretical value in the infinitely deep surrounding fluid is equal to $\sqrt{2}$; according to the data of recent paper [4], it equals 1 that coincides with our result.

Universality both of the local Fr number and the very gravity current features is manifested only in the infinitely deep surrounding fluid. In a general case, the gravity current features depend also on the height of the surrounding fluid in which it propagates, in this paper – on the atmosphere height H. If the parameter D/H is not very small, dependence of the gravity current features upon it is rather substantial [4, 5]. In our experiments, this parameter took on the values with in the range $0.2 < D/H < 0.4$ (Table 3). In this range, though finiteness of the atmosphere height affects the gravity current features, it is rather weak.

Let us compare our results with those in other studies which took into consideration the finite value of H. First of all, let us calculate the theoretical value of the local Fr for the finite atmosphere height, according to [4], since [4] gives the Froude number values calculated using the height H (in the present paper they are calculated using h):

$$\mathrm{Fr}_{\mathrm{theor}} = \sqrt{\frac{(D-h)(H-h)}{Hh}}. \tag{11}$$

The calculated theoretical values $\mathrm{Fr}_{\mathrm{theor}}$ (Table 1 and 2) slightly exceed Fr_h that can be due to presence of dissipation in the numerical experiments.

In [4, 5, 7] that take into account finiteness of H, Fr_D calculated based on the cold pool initial height D is used. Compare the results of the above-mentioned papers with the data in Table 3. Fig. 6, *a* in [5] represents dependences of Fr_D upon the parameter D/H obtained both theoretically and numerically. The analogous dependences are shown in Fig. 14 in [4]. Comparison of the data in the seventh column of Table 3 with the indicated figures (the D/H values vary from 0.2 to 0.4) demonstrates good agreement between the results: the Froude number slowly decreases with increase of the parameter D/H.

Another important result which can be obtained from our numerical experiments consists in determining the dependence of the gravity current height h_1 on the pool initial height D. The graph of the dependence of the ratio h_1/D on the parameter D/H is shown in Fig. 6, *b* in [5]. For small values of D/H, this dependence is rather weak. Within the infinite depth H, the ratio h_1/D takes on the value 0.347. According to the data from Table 3 for three numerical experiments, the ratio h_1/D takes on the values 0.37, 0.39 and 0.40 that is in agreement with the mentioned figure from [5].

Thus, all the gravity currents' characteristics calculated in the present paper using the full two-dimensional atmosphere hydrodynamic model with high resolution are in quantitative agreement with the previous results.

5. Conclusion

Propagation of a gravity current in the atmosphere is numerically simulated in the present paper. It was done using the two-dimensional full hydrodynamic model of the compressible atmosphere at high spatial resolution. Development of the gravity current at the stage of the constant front speed is completely described in details. Considered and described are spatial distribution and temporal evolution of all the dynamic variables in the very gravity current and in the surrounding atmosphere, i.e. potential temperature and two components of velocity and pressure.

Formation of the characteristic features of the gravity current structure – the front, the “head”, the Kelvin – Helmholtz vortices is noted.

Dependence of the current characteristics upon two parameters – the initial difference between the potential temperatures of the cold air area and the environment and also the cold area initial height is considered. The Froude number was taken as the main quantitative characteristic of the gravity current. It was calculated by three methods: using the characteristic heights of the current “head” and “body”, and the cold pool initial height. It is revealed that in the first approximation, the Froude number calculated by the gravity current height is a universal constant approximately equal to 1. The more detailed analysis permitted to conclude that the ratio of the cold pool initial height to the atmosphere thickness weakly affects the Froude number and the gravity current height. It is consistent with the results of other researches.

REFERENCES

1. Haase, S.P., Smith, R.K., 1989, “The numerical simulation of atmospheric gravity currents. Part I: Neu-trally-stable environments”, *Geophys. Astrophys. Fluid Dyn*., vol. 46, no. 1-2, pp. 1-33.
2. Rottman, J.W., Simpson, J.E., 1983, “Gravity currents produced by instantaneous releases of a heavy fluid in a rectangular channel”, *J. Fluid Mech*., vol. 135, pp. 95-110.
3. Marino, B.M., Thomas, L.P. & Linden, P.F., 2005, “The front condition for gravity currents”, *J. Fluid Mech.*, vol. 536, pp. 49-78.
4. Shin, J.O., Dalziel, S.B. & Linden, P.F., 2004, “Gravity currents produced by lock exchange”, *J. Fluid Mech*., vol. 521, pp. 1-34.
5. Klemp, J.B., Rotunno, R. & Skamarock, W.C., 1994, “On the dynamics of gravity currents in a channel”, *J. Fluid Mech*., vol. 269, pp. 169-198.
6. Droegemeier, K.K., Wilhelmson, R.B., 1987, “Numerical simulation of thunderstorm outflow dynamics. Part I: Outflow sensitivity experiments and turbulence dynamics”, *J. Atmos. Sci*., vol. 44, iss. 8, pp. 1180-1210.
7. Benjamin, T.B., 1968, “Gravity currents and related phenomena”, *J. Fluid Mech*., vol. 31, no. 02, pp. 209-248.
8. Ungarish, M., 2010, “An introduction to gravity currents and intrusions”. Boca Raton, CRC Press, Taylor and Francis Group, 512 p.
9. Dailey, P.S., Fovell, R.G., 1999, “Numerical simulation of the interaction between the sea-breeze front and horizontal convective rolls. Part 1: Offshore ambient flow”, *Mon. Wea. Rev*., vol. 127, no. 5, pp. 858-878.